Accuracy analysis of screen propagators for wave extrapolation using a thin-slab model

Ru-Shan Wu, Institute of Tectonics, University of California, Santa Cruz, CA; Maarten V. de Hoop, Center for Wave Phenomena, Colorado School of Mines, Golden, CO*

Summary

One-way wave extrapolators, such as the split-step Fourier method, generalized screen methods including the phase-screen, complex screen and wide-angle screen methods, have been proposed recently as part of the solution to lessen the CPU and memory size requirement of wave equation based 3D subsurface imaging methods. The phase space path-integral formulation and the vertical slowness symbol analysis provide a general and convenient background for the accuracy estimation of screen propagators. By comparing the dispersion relations of screen propagators in the h-f limit with the leading term h-f asymptotics to the vertical slowness symbol, and through numerical experiments of thin-slab transmission, it is seen that for weak perturbations both phase-screen and wide-angle screen propagators perform well; While for the case of strong medium contrasts, the modified wide-angle screen propagator has much better accuracy. The screen propagators have great potential in the application to 3D prestack depth migration as extrapolators.

Introduction and Theory

The requirement for huge CPU time and memory size by 3D wave extrapolators prevents the practical use of wave equation based methods to the 3D subsurface imaging, such as the prestack depth migration. One-way wave extrapolators, such as the split-step Fourier method (Stoffa et al., 1990), generalized screen method including the phase-screen, complex screen and wide-angle screen methods (Wu, 1994; Wu and Xie, 1994; Wu and Huang, 1995) have been proposed recently as part of the solution. However, the accuracy and angular dependence of accuracy have not been thoroughly studied. In this study we will adopt a phase-space path integral formulation and perform the the vertical slowness pseudo-differential operator analysis using a thin-slab model to demonstrate the angular dependencies of various generalized screen propagators.

One-Way Wave Propagation in the Form of Path-Integral

The solution of the one-way acoustic wave equation can be represented by a Hamiltonian path-integral (phase space or "dual-domain" path-integral) (Fishman and McCoy, 1984; de Hoop, 1996; de Hoop and Wu, 1996):

$$\mathcal{G}^{(+)}(\mathbf{x}_T, z; \mathbf{x}'_T, z') = H([z-z']) \int_P \mathcal{D}(\mathbf{x}''_T, \boldsymbol{\alpha}''_T)$$
$$\exp\left[i\omega \int_{\zeta=z'}^{z} \mathrm{d}\zeta \{ i\boldsymbol{\alpha}''_T \cdot (d_\zeta \mathbf{x}''_T) + \gamma^{(+)}(\mathbf{x}''_T, \zeta, \boldsymbol{\alpha}''_T)\} \right] \quad (1)$$

where $\boldsymbol{\alpha}_T$ is the transverse slowness vector and is related with the horizontal wavenumber $\mathbf{K}_T$ by $\mathbf{K}_T = \omega\boldsymbol{\alpha}_T$, $H()$ is the Heaviside function, $\mathcal{D}(\mathbf{x}''_T, \boldsymbol{\alpha}''_T)$ is a measure of the "width" of path $(\mathbf{x}''_T, \boldsymbol{\alpha}''_T)$, and P is a set of paths $(\mathbf{x}''_T(\zeta), \boldsymbol{\alpha}''_T(\zeta))$ in the (horizontal) phase space. In Eq.(1) $\gamma^{(+)}$ is the left symbol of the vertical slowness operator $\Gamma^{(+)}$ (a square-root operator), which is defined By letting the operator Γ act on a Fourier component $\exp(i\omega\boldsymbol{\alpha}_T \cdot \mathbf{x}_T)$

$$\Gamma(\mathbf{x}_T, \nabla_T)\, e^{(i\omega\boldsymbol{\alpha}_T\cdot\mathbf{x}_T)} = \gamma(\mathbf{x}_T, \boldsymbol{\alpha}_T) e^{(i\omega\boldsymbol{\alpha}_T\cdot\mathbf{x}_T)}\,. \quad (2)$$

In the case of lateral homogeneity, $\gamma(\mathbf{x}_T, \boldsymbol{\alpha}_T)$ does not depend on $\mathbf{x}_T$, then $\gamma = \gamma(\boldsymbol{\alpha}_T) = [(1/c)^2 - \alpha_T^2]^{1/2}$ becomes the scalar vertical slowness and the path-integral (1) reduces to the phase-shift extrapolator in homogeneous media. If we know the exact form of the vertical slowness left symbol (VSLS) $\gamma(\mathbf{x}_T, \boldsymbol{\alpha}_T)$ for a general inhomogeneous medium, we would be able to march the one-way wave forward precisely, although the process might be very computationally intensive. Unfortunately, no general solution exists or is expected to come into exist soon. We have to rely on asymptotic analysis of operator symbols and various approximation techniques.

Approximate VSLS by screen propagators

Assuming that a VSLS (vertical slowness left symbol) can be approximated by a laterally homogeneous vertical slowness $\gamma_0(\boldsymbol{\alpha}_T)$ plus a small perturbation operator $\eta(\mathbf{x}_T, \boldsymbol{\alpha}_T)$,

$$\gamma(\mathbf{x}_T, \boldsymbol{\alpha}_T) \approx \gamma_0(\boldsymbol{\alpha}_T) + \eta(\mathbf{x}_T, \boldsymbol{\alpha}_T) \quad (3)$$

Compared with Wu and Huang (1995)'s dual-domain expression for wide-angle thin-slab scattering in acoustic media (equation 18), we find

$$\eta^{WH}(\mathbf{x}_T, \boldsymbol{\alpha}_T) = \alpha_0(\frac{\alpha_0}{\gamma_0})\frac{1}{2}\left[\varepsilon_\kappa(\mathbf{x}_T) + \frac{i}{\omega\alpha_0}\hat{\boldsymbol{\alpha}}\cdot\varepsilon_\rho(\mathbf{x}_T)\nabla\right] \quad (4)$$

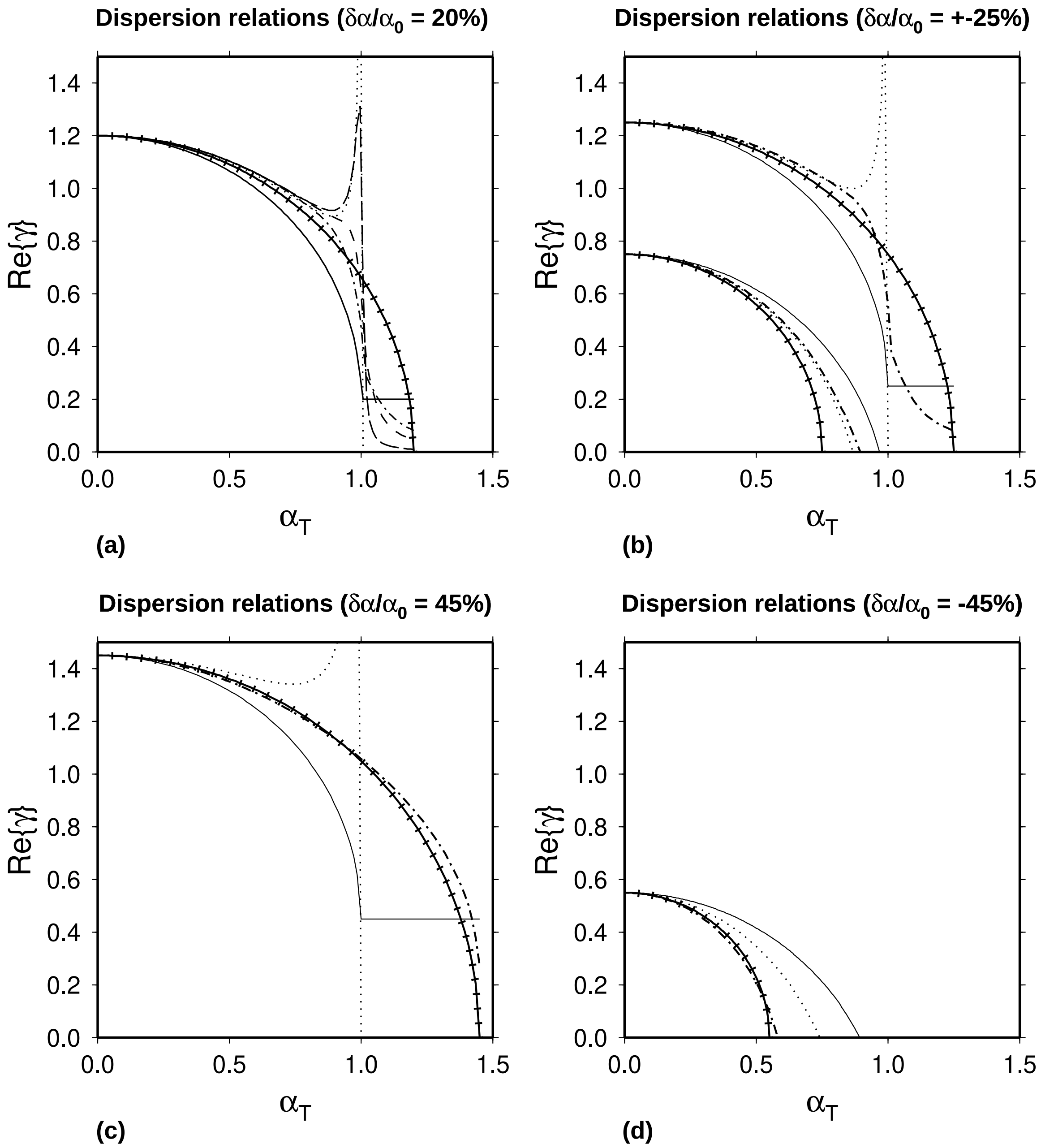

Figure 1: Dispersion relations of wide-angle screen propagators in the high frequency limit. As references, the exact h-f curves are shown in ticked solid lines; the curves for phase-screen are solid lines. The dotted lines are for the original wide-angle screens. The others are for the modified wide-angle screens:

(a) The case of complex $\gamma_2 = \sqrt{\alpha_0 - (\xi\alpha_T)^2}$ with $Re(\xi) = 1$ and $Im(\xi) = 0.01$ for the long dashed line, 0.05 for dashed line, 0.1 for dotted-dashed line.

(b) The case of complex γ_2 with $\xi = 1 + 0.1i$ for $\delta\alpha/\alpha_0 = \pm 25\%$

(c) The case of stretched γ_1 and γ_2 with $b = 0.7, \xi = 0.08 + 0.9i$ for $\delta\alpha/\alpha_0 = 45\%$

(d) The case of stretched γ_1 and γ_2 with $b = 1.6, \xi = 0.1 + 1.0i$ for $\delta\alpha/\alpha_0 = -45\%$

where $\alpha_0 = 1/c$ is the background slowness and $\hat{\boldsymbol{\alpha}}$ is the unit slowness direction vector. For media with constant density, it becomes the formulation for scalar wave equation. The corresponding symbol reduces to

$$\eta^{WS}(\mathbf{x}_T, \boldsymbol{\alpha}_T) = \alpha_0(\frac{\alpha_0}{\gamma_0(\boldsymbol{\alpha}_T)})S_v(\mathbf{x}_T) \quad (5)$$

with

$$S_V(\mathbf{x}_T) = \frac{1}{2}\frac{\alpha^2(\mathbf{x}_T) - \alpha_0^2}{\alpha_0^2} \approx \frac{\alpha(\boldsymbol{\alpha}_T) - \alpha_0}{\alpha_0} = \frac{\delta\alpha}{\alpha_0} \quad (6)$$

Because $\eta(\mathbf{x}_T, \boldsymbol{\alpha}_T)$ is separable with respect to $\mathbf{x}_T$ and $\boldsymbol{\alpha}_T$, therefore the thin-slab propagation can be implemented by a dual-domain technique using FFT. The phase-screen propagator approximates $\eta(\mathbf{x}_T, \boldsymbol{\alpha}_T)$ with $\eta(\mathbf{x}_T)$, which gains further computational advantages. The phase-screen approximation leads to

$$\gamma^{PS}(\mathbf{x}_T, \boldsymbol{\alpha}_T) = \gamma_0 + \alpha_0 S_v(\mathbf{x}_T) \quad (7)$$

a total split of slowness domain and space domain operations.

Accuracy analysis for screen propagators

The comparison of accuracies between the screen propagators and the high-frequency asymptotics is not quite a fair comparison, since the two have quite different ranges of validity. When the frequency approaches to infinity, the h-f asymptotics becomes more accurate, but the perturbation solutions remain approximate. On the other hand, when the wavelength of the wave field is comparable to the scales of lateral heterogeneities, the h-f asymptotics becomes less accurate while the perturbation methods may remain in the valid region. However, since the eikonal equation of a wave field in smooth media behaves similar to h-f asymptotics, it will be instructive to perform the comparison for understanding the errors of screen extrapolators at high-frequencies.

Fig. 1 shows the dispersion relations of screen propagators in the h-f limit compared with the leading term of h-f asymptotics which is considered as "exact" in the h-f limit and shown in ticked solid lines as references. The dotted lines are for the original wide-angle screens and the solid lines are for the phase-screens. The horizontal axes are the transverse slowness, and the vertical axis, the real part of vertical slowness. We see that, such as in Fig. 1a, the wide-angle screen propagator is more accurate than the phase-screen propagator but has a pole near the critical angle. This only happens for low velocity perturbations. Around the pole, the vertical slowness increases drastically, which can cause numerical dispersions and instability. In order to overcome the pole problem, we introduce a modified wide-angle VSLS:

$$\gamma^{WSC} = \gamma_1(\boldsymbol{\alpha}_T) + \delta\alpha(\alpha_0/\gamma_2(\boldsymbol{\alpha}_T))$$

$$\begin{aligned}\gamma_1 &= \sqrt{\alpha^2 - (b\alpha_T)^2} \\ \gamma_2 &= \sqrt{\alpha_0^2 - (\xi\alpha_T)^2}\end{aligned} \quad (8)$$

where b is a real number and ξ is a complex number. To improve the behavior of γ^{WS} near the pole, we need only put a small imaginary part to ξ. Fig. 1a is the case of complex γ_2 The perturbation is $\delta\alpha/\alpha_0 = \pm 20\%$. We see that not only the pole is removed but the accuracies at large angles are also improved. Fig. 1b is the case of complex γ_2 with $\xi = 1 + 0.1i$ for $\delta\alpha/\alpha_0 = \pm 25\%$, which corresponding the practical velocity contrast for salt-dome structures having velocity $4000m/s$ of salt-dome and $2200m/s$ for the host medium. if we take the median slowness as the background slowness, the dispersion relations of the complexified wide-angle propagator are shown as the dotted-dashed lines for the salt (-25% perturbation) and the host medium ($+25\%$ perturbation). The response of γ^{WSC} to the high velocity perturbation is similar to γ^{WS}, but the pole of the low velocity perturbation response has been effectively removed. As shown later in the numerical experments of thin-slab transmission, the stability has been significantly improved (Fig. 2b). Fig. 1c and d show the combining effect of wavenumber stretching and complexification. Although the exact dispersion relations can be matched very well for such high velocity contrasts by optimizing the stretching and attenuating factors, the optimal match is strongly contrast dependent.

To test the real performance of screen propagators in laterally heterogeneous media with strong velocity contrast, we use a thin-slab with a ramp velocity model as shown in the top panels of Fig. 2. This ramp model simulate the transition of medium velocity from the salt dome to the host medium or vice versa. In Fig. 2a Velocity jumps from 2200 m/s to 3000 m/s while in 2b, jumps from 2200 m/s to 4000 m/s. Plane waves are incident on the thin-slab with different incident angles. In 2a, the corresponding incident angles are 50^o and 34^o for the two velocities respectively. $\Delta\tau^{PS}$ is the time delays calculated by the phase screen propagator; $\Delta\tau^{WS}$ is that by the wide-angle screen propagator with real γ_2; $\Delta\tau^{WSC}$ is that with complex γ_2. The dotted lines are the geometric optics predictions as references. We see the excellent performance of the wide-angle screen propagators (the third and the fourth panels) compared to the phase-screen propagator (the second panel). Note also that the regular wide-angle screen propagator has some instability problem caused by the pole, as shown by the rings on the curve. This instability is largely removed by the complex γ_2. Fig. 2b shows the case of strong contrast and large incident angle ($\theta_1 = 65^0$). The accuracy of the modified wide-angle screen propagator (the fourth panel) is still reasonably good.

Conclusions

The phase space path-integral formulation and the vertical slowness symbol analysis provide a general and convenient background for the accuracy estimation of screen propagators. By comparing the dispersion relations of screen propagators in the h-f limit with the leading term h-f asymptotics to the vertical slowness symbol, and through numerical experiments of thin-slab transmission, we see that for weak perturbations both phase-screen and wide-angle screen propagators perform well; While for the case of strong medium contrasts, the pole-removed wide-angle screen propagator with complex $gamma_2$ has much better accuracy than the phase-screen. Therefore, with some improvements the screen propagators have great potential in the application to 3D prestack depth migration as extrapolators.

Acknowledgements

The support from the ACTI project of UCSC granted from the United States Department of Energy administered by the Los Alamos National Laboratory and the support from the W. M. Keck Foundation are acknowledged. Contribution number 299 of the Institute of Tectonics, University of California, Santa Cruz,

References

De Hoop, M.V., 1996, Generalization of the Bremmer coupling series, *to appear in* J. Math. Phys..

De Hoop, M.V., and Wu, R.S., 1996, General formulation and accuracy of the complex screen method, *submitted to* Wave Motion.

Fishman, L., and McCoy, J.J., 1984, Derivation and application of extended parabolic wave theories II. Path integral representations, J. Math. Phys., **25** 297-308.

Stoffa, P. L., Fokkema, J. T., de Luna Freire, R. M., and Kessinger, W. P., 1990, Split-step Fourier migration: Geophysics, **55**, 410–421.

Wu, R.S., 1994. Wide-angle elastic wave one-way propagation in heterogeneous media and an elastic wave complex-screen method, *J. Geophys. Res.*, **99**, 751-766.

Wu, R.-S., and Huang, L.-J., 1995, Reflected wave modeling in heterogeneous acoustic media using the de Wolf approximation: *in* S. Hassanzadeh, Editor, Mathematical Methods in Geophysical Imaging III, Proc. SPIE **2571**, 176-186.

Wu, R.-S., and Xie, X.-B., 1994, Multi-screen backpropagator for fast 3D elastic prestack migration, *in* S. Hassanzadeh, Editor, Mathematical Methods in Geophysical Imaging II, Proc. SPIE **2301**, 181-193..

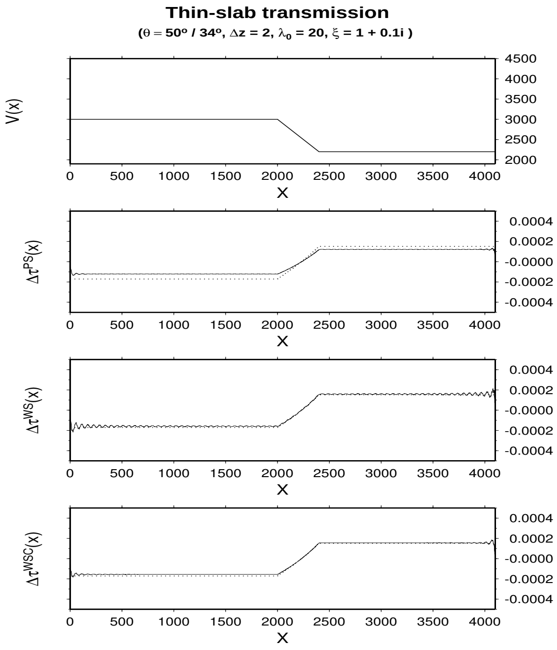

(a)

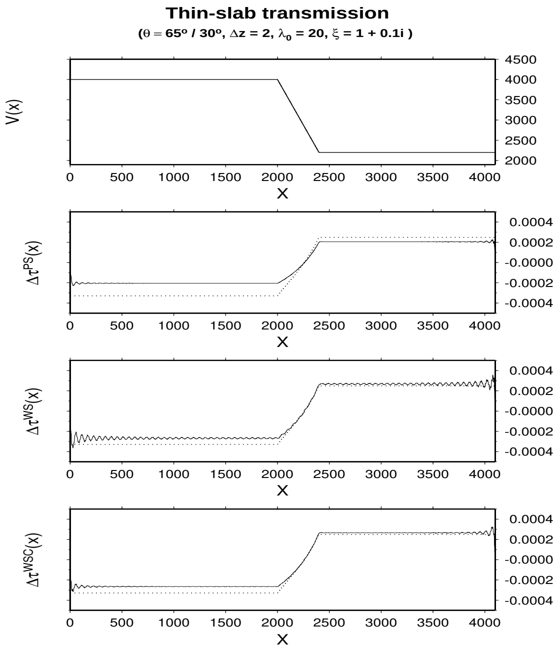

(b)

Figure 2: Thin-Slab transmission tests using different screen propagators. The top panel is the velocity model. $\Delta\tau^{PS}$ is the time delay calculated by the phase screen propagator; $\Delta\tau^{WS}$ is that by the wide-angle screen propagator with real γ_2; $\Delta\tau^{WSC}$ is that with complex γ_2. The dotted lines are the geometric optics predictions.
(a) Velocity jumps from 2200 m/s to 3000 m/s ($\theta_1 = 50^0$)
(b) Velocity jumps from 2200 m/s to 4000 m/s ($\theta_1 = 65^0$)
It can be seen that the wide-angle screen propagator with complex γ_2 has the best results.